

Suggested Correlation between the Visible Photoluminescence and the Fourier Transform Infrared Spectrum of a Porous Silicon Surface

James L. Gole*

School of Physics, Georgia Institute of Technology, Atlanta, Georgia 30332

David A. Dixon

Environmental Molecular Sciences Laboratory, Pacific Northwest National Laboratory, P.O. Box 999, K1-83, Richland, Washington 99352

Received: April 4, 1997; In Final Form: May 27, 1997[®]

The FTIR spectrum for a heavily oxidized porous silicon (PS) surface is considered. It is suggested that a portion of this spectrum be reassigned to the Si=O stretch frequency of a surface bound-silanone-based silicon oxyhydride consistent also with the ¹⁸O₂/¹⁶O₂ isotopic labeling of the FTIR spectrum and with matrix isolation infrared spectra for silanone, silanoic acid, and silicic acid. Within the framework of this assignment the FTIR spectrum, the photoluminescence excitation spectrum, and the visible photoluminescence spectrum of PS correlate well with a surface-bound silanone-based silicon oxyhydride fluorophor.

Introduction

The discovery of room temperature visible luminescence¹ from high surface area porous silicon (PS) structures formed in wafer scale, through electrochemical etching, has attracted considerable interest primarily because of its potential use in the development of silicon based optoelectronics, displays, and sensors. While the luminescence is thought to occur near the silicon surface,^{2,3} the source of the luminescence is controversial because the efficiency and wavelength range of the emitted light can be affected by the physical and electronic structure of the surface, the nature of the etching solution,^{4,5} and the nature of the environment in which the etched sample is placed. Here, we make use of recent experiments⁶ and detailed quantum chemical modeling⁷ conducted in our laboratories to suggest a correlation between the visible photoluminescence characteristic of a porous silicon surface and the FTIR spectra^{8–12} observed to characterize this surface. We suggest an alternate assignment for certain features observed in the infrared absorption spectrum simultaneously consistent with the isotope effect,¹² the photoluminescence excitation spectrum (PLE),¹³ and the visible photoluminescence spectrum^{6,7} of porous silicon.

The most widely considered hypothesis to explain the luminescence from PS suggests that it results from the radiative recombination of quantum-confined electrons and holes in columnar structures or undulating wires.^{14–16} It has also been suggested that surface localized states, involving irregularly shaped small crystallites that are not perfectly passivated, produce elementary excitations which are first trapped prior to recombination.^{8,17} Yet a third explanation contends that the luminescence results from the presence of surface confined molecular emitters. These include polysilane¹⁸ and siloxene (Si₆O₃H₆) and its derivatives.^{19–21} Stutzmann and co-workers^{19–21} using the optical detection of magnetic resonance (ODMR) have established that the PS “red” emission results from a triplet exciton suggesting that this exciton corresponds to an annealed siloxene molecule. We have recently suggested a more general origin for the observed features^{6c,e,7} which concurs with Steckl et al.²² who first obtained evidence for the silicon oxyhydrides in stain etched porous silicon thin films, correlating their

observations with crystallinity and photoluminescence, while Yan et al.²³ suggested that SiOH could be found on the PS surface.

There has been considerable effort to correlate the PL from porous silicon with changes in the PS surface using FTIR spectroscopic techniques to follow the oxidation cycle.^{8–12} In the course of their studies Xie et al.⁸ have obtained FTIR spectra for PS films, both freshly prepared and aged in air. Upon aging, a broad feature, which has been associated with the Si–O–Si moiety at $\nu \sim 1100 \text{ cm}^{-1}$, grows and eventually dominates the spectrum. A similar behavior has been observed by Hory et al.⁹ in their monitoring of PS passivation. Furthermore, Dubin et al.,¹¹ during the activation period for the corresponding electroluminescence, observe the growth of features in the 1050–1250 cm^{-1} region which they also assign to ν (Si–O–Si). Most recently Mawhinney et al.¹² have carried out an elegant and detailed FTIR study of the oxidation of PS observing not only the broad $\sim 1100 \text{ cm}^{-1}$ feature, which they also attribute to ν (Si–O–Si), but also clear spectral features associated with ν (Si–O–H) and ν (–O_{*y*}Si–H_{*x*}). Here, we will offer an alternate assignment for at least a significant portion of the 1100 cm^{-1} region,^{6c,7} consistent with the electronic spectroscopy of the PS surface and associated with the formation of the silanone based silicon oxyhydrides.

We have carried out an extensive series of experiments⁶ in both aqueous (HF/H₂O, HF/CH₃OH/H₂O, HF/C₂H₅OH/H₂O, and HF/H₂O/HCl) and nonaqueous (MeCN/HF) (anhydrous)) etching media, monitoring the time dependent PL both in situ (during the etching cycle and before the PS sample is removed from the etching solution) and ex situ (after removal of the PS from the etching solution). By correlating the ex-situ and in-situ behavior of the PS, we find evidence which supports a surface bound molecule-like emitter as the source of the PL from porous silicon.⁶ Several observations lead us to this conclusion. We observe the early appearance in time (<10 s) of the PS luminescence consistent with the formation of a surface-bound emitter created on a time scale much shorter than that necessary for pore formation.⁶ We find that a selection of laser excitations (PLE) over the wavelength range extending from 193 to 400 nm produce an almost identical *time dependent* PL emission feature.^{6c} These results, which are not consistent

[®] Abstract published in *Advance ACS Abstracts*, July 15, 1997.

with quantum confinement, suggest the pumping of the excited state manifold of a molecule-like species followed by rapid nonradiative vibrational relaxation through this manifold and the subsequent emission of radiation at much longer wavelength.

Experiments, as supported by detailed quantum chemical modeling,⁷ suggest a correlation of the porous silicon PL with the manifold of low-lying electronic states associated with the silanone based silicon oxyhydrides of the form $\text{O}=\text{Si}-\text{OH}$ ^{22,23} or $\text{O}=\text{Si}-\text{OSiH}_3$. Changes in bonding associated with electronic transitions involving the oxyhydride ground electronic and low-lying triplet states,²¹ especially in the SiO related bonds, and the substantial shift to larger internuclear distance of these excited electronic states relative to their ground states can readily explain the observed character of the PL spectra. The excitation to a manifold of states greatly shifted from the ground electronic state partially explains the significant red shift of the PL spectrum (600–800 nm) from the known absorption peak wavelength of the (PLE) excitation spectrum (~ 350 nm).¹³ In concert with these observations is the reassignment of features in the 1100–1250 cm^{-1} infrared spectral region at least in part to an Si=O stretch.

Correlation of Experimental Results and Quantum Chemical Modeling

FTIR Spectrum of a Porous Silicon Surface. Mawhinney et al.¹² have used FTIR spectroscopy to study the oxidation of porous silicon in studies employing isotopically labeled oxygen and hydrogen/deuterium. These authors used boron doped p-type Si(100) crystals which, after careful cleaning using the RCA procedure,²⁴ they have anodically etched in “deoxygenated” aqueous solutions of 48% HF (aq) and anhydrous ethanol. The etched crystal was dipped in concentrated HF to remove surface oxides and residual etching solution before its mounting into an infrared cell. $^{16}\text{O}_2$ (Matheson, 99.998%), $^{18}\text{O}_2$ (ICON Services, 95% isotopic purity), and D_2 (Matheson, 99.82 atom%) were transferred to the cell for isotopically labeling the oxidation of the hydrogen terminated PS surfaces. Mawhinney et al.¹² obtained and compared infrared absorption spectra in the range 500–4000 cm^{-1} for their silicon crystals, freshly prepared porous silicon, and both partially and heavily oxidized porous silicon. All spectra were recorded with computer control at 2 cm^{-1} resolution and averaged using the data from 1024 scans. In the course of these studies, Mawhinney et al. first observed surface features on the freshly formed porous silicon surface attributable to SiH_x which transform on oxidation to $\text{O}_y\text{Si}-\text{H}_x$ constituencies. Further oxidation also reveals the previously observed broad emission feature in the region of the 1108 cm^{-1} bulk Si–O–Si mode. We depict their ^{18}O - and ^{16}O -labeled spectra (oxidation with $^{18}\text{O}_2$ and $^{16}\text{O}_2$) in Figure 1. Mawhinney et al. use their data to demonstrate that the crystals used in their study contain oxygen in the bulk as evidenced by the 1108 cm^{-1} absorbance, which in this overlapped region is shifted to the features at 1125 and 1134 cm^{-1} . They find that the absorbance in this region grows with continued oxidation, encompassing the range from 1250 cm^{-1} to 950 cm^{-1} , but *never* merges with the bulk Si–O–Si bands. These bands do not shift with $^{18}\text{O}_2$ oxidation, suggesting that they are not related to the surface oxidation process. While the features in Figure 1 have been assigned to a surface Si–O–Si constituency,¹² we will offer an alternate interpretation consistent also with the experimentally observed isotope effect.

Finally, Mawhinney et al. observe the development of an SiO–H stretch mode whose $^{16}\text{O}/^{18}\text{O}$ substituted features are depicted in Figure 2. Their observations confirm the results of Steckl et al.²² and Yan et al.²³ The observed frequency shifts

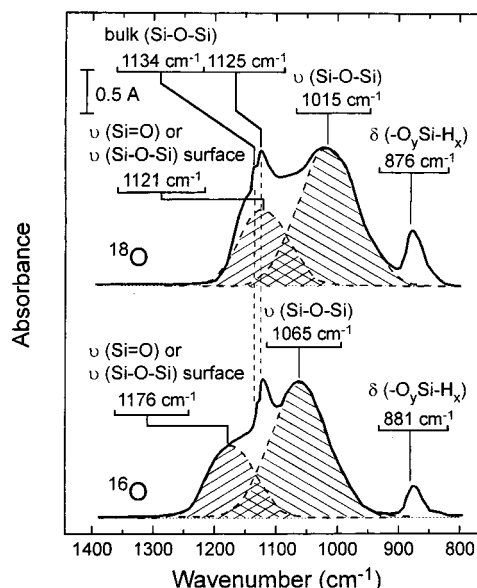


Figure 1. Silicon oxide mode structure measured at 108K after oxidation of a porous silicon surface with $^{16}\text{O}_2$ and $^{18}\text{O}_2$. The cross-hatched absorbance bands identified by Mawhinney et al. (ref 12) are reassigned to silicon–oxygen based surface vibrations belonging to Si=O stretching and Si–O–Si skeletal modes. The suggested assignment of the Si=O band represents a deviation from ref 12.

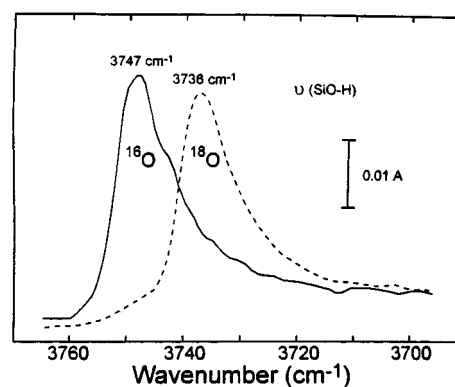


Figure 2. Isotopic frequency of the SiO–H stretch for oxidation with $^{16}\text{O}_2$ and $^{18}\text{O}_2$ (after ref 12).

between $^{16}\text{O}_2$ and $^{18}\text{O}_2$ oxidized porous silicon are indicated in Table 1. It is noteworthy that, on the basis of the observed isotope shifts, Mawhinney et al. assign the ubiquitous 880 cm^{-1} band to an oxidized hydride deformation mode associated with the $-\text{O}_y\text{Si}-\text{H}_x$ constituency. They note, however, that this warrants further discussion.

Quantum Chemical Modeling. Electronic Spectroscopy. In order to assess whether the source of the PS photoluminescence could be a silicon oxyhydride-like fluorophor strongly bound to the PS surface, we have carried out a detailed quantum chemical study⁷ of several model compounds. We have employed both ab-initio molecular orbital theory and density functional theory (DFT). The calculations have been done using the program systems DGAuss²⁵ (DFT calculations) and Gaussian 94²⁶ (ab-initio MO calculations). The molecules $\text{Si}(\text{O})\text{H}_2$, $\text{Si}(\text{O})\text{H}(\text{OH})$, $\text{Si}(\text{O})(\text{OH})_2$, $\text{Si}(\text{O})\text{H}(\text{OSiH}_3)$, $\text{Si}(\text{O})\text{H}(\text{SiH}_3)$, $\text{Si}(\text{O})(\text{OH})(\text{SiH}_3)$, and $\text{Si}(\text{O})(\text{SiH}_3)_2$ were used as models for the various sites that might be present on a hydrogen-passivated silicon surface²⁷ undergoing oxidation. The first three of these, silanone, silanoic, and silicic acid, have also been isolated in rare gas matrices²⁸ and portions of their infrared spectra recorded. Although cluster models such as those which we consider do not include the long range Coulomb effects present in the bulk,

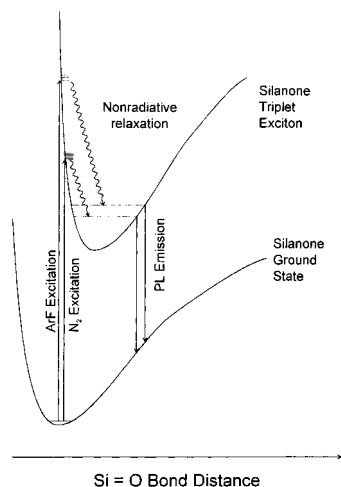


Figure 3. Schematic of silicon oxyhydride ground state singlet and excited state triplet potentials indicating (1) the possible origin of the substantial difference in photoluminescence excitation (PLE) and subsequent photoluminescence (PL) emission energies and (2) the distinction between an ArF excimer laser and nitrogen laser pump of a porous silicon sample. Laser pumping is followed by fast nonradiative vibrational relaxation within the excited state triplet manifold and subsequent emission of radiation at much longer wavelength than that corresponding to the pump energy.

TABLE 1: FTIR Absorption Frequencies for $^{16}\text{O}_2$ - and $^{18}\text{O}_2$ -Oxidized Porous Silicon Surfaces^a

vibrational mode assignment	observed frequency (cm ⁻¹) $^{16}\text{O}_2$	observed frequency (cm ⁻¹) $^{18}\text{O}_2$
$\nu(\text{Si}-\text{OH})^b$	3747	3736
$\nu(-\text{O}_2\text{Si}-\text{H}_x)$	2273	2271
$\nu(\text{Si}-\text{O}-\text{Si})^c$	1176	1121
$[\nu(\text{Si}=\text{O})]$		
$\nu(\text{Si}-\text{O}-\text{Si})^c$	1065	1015
$\delta(-\text{O}_2\text{Si}-\text{H}_x)^c$	881	876

^a From ref 12. ^b See Figure 2. ^c See Figure 1.

they can provide useful insights into the effect of changing the functional groups which are attached to the silicon.

Geometries for the ground state singlet structures were initially optimized using polarized triple- ζ valence basis sets²⁹ at the local DFT level. Second derivative calculations³⁰ on the optimized structures showed them to be minima. Geometries for the first excited triplet state of a selection of the molecules considered were also optimized at this level. The optimum DFT geometries were then used in molecular orbital calculations at the MP2 level³¹ with a polarized double- ζ basis set.³² The geometries were again optimized at the MP2/DZP level and frequency calculations were done for these optimized geometries. The open shell ab-initio MO calculations were carried out using the UHF formalism. Higher order correlation calculations were done on $\text{Si}(\text{O})\text{H}_2$ at the optimized geometries. These calculations were done at the CCSD(T) level³³ with a triple- ζ basis set³⁴ augmented by two sets of polarization functions on all atoms and by f functions on the heavy atoms.

The most relevant results of these calculations are summarized in Tables 2 and 3. A detailed description is given elsewhere.⁷ In Table 2 we summarize the $\text{Si}=\text{O}$ bond lengths determined for the ground state singlet and low-lying excited state triplet of the model compounds considered. The calculated $\text{Si}=\text{O}$ bond lengths are slightly longer than the 1.509 739 Å bond length³⁵ for the ground electronic state of $\text{Si}=\text{O}$. The calculations demonstrate a significant change in the excited triplet state bonding relative to the ground state, localized largely in the SiO bonds. The predicted considerable increase in the SiO bond length, paralleled by a considerable decrease in the “ $\text{Si}=\text{O}$ ”

TABLE 2: $\text{Si}=\text{O}$ Bond Lengths (Å) for Silanones at the MP2/DZP Level

molecule	$r(\text{Si}-\text{O})$ singlet	$r(\text{Si}-\text{O})$ triplet	$\Delta r(\text{Si}-\text{O})$
$\text{Si}(\text{O})\text{H}_2$	1.545	1.700 ^a	0.155
$\text{Si}(\text{O})\text{H}(\text{OH})^b$	1.537	1.709	0.172
$\text{Si}(\text{O})(\text{OH})_2$	1.536	1.709	0.173
$\text{Si}(\text{O})\text{H}(\text{OSiH}_3)$	1.537	1.708	0.171
$\text{Si}(\text{O})\text{H}(\text{SiH}_3)$	1.553	1.695	0.142
$\text{Si}(\text{O})(\text{OH})(\text{SiH}_3)$	1.543	1.712	0.169
$\text{Si}(\text{O})(\text{SiH}_3)_2$	1.560	1.681	0.121

^a Bond length for the excited singlet is 1.705 Å. ^b Bond lengths for $\text{HO}-\text{Si}-\text{OH}$ silylene are 1.670 Å for the ground state singlet and 1.680 Å for the excited triplet.

TABLE 3: Ground State Singlet–Excited Triplet Energy Separation for Silanones (Silylenes)

molecule	$\Delta E(\text{S}-\text{T})$ kcal/mol	$\Delta E(\text{S}-\text{T})$ eV	$\sim \lambda_{\text{adiabatic}}$ (nm)
$\text{Si}(\text{O})\text{H}_2$	60.1	2.61	475
$\text{Si}(\text{O})\text{H}(\text{OH})$	70.9	3.07	403
$\text{Si}(\text{O})(\text{OH})_2$	71	3.08	402
$\text{Si}(\text{O})\text{H}(\text{OSiH}_3)$	70.3	3.05	406
$\text{Si}(\text{O})(\text{OH})(\text{SiH}_3)$	71.2	3.09	401
$\text{Si}(\text{O})\text{H}(\text{SiH}_3)$	57.3	2.48	499
$\text{Si}(\text{O})(\text{SiH}_3)_2$	53.9	2.34	530
HSiOH	38.4	1.66	744
HOSiOH	64.2	2.78	445
SiH_3OSiOH	67.3	2.92	425

stretch frequency of the excited triplet state⁷ closely follows the pattern of the known intercombination band systems of $\text{SiO}^{7,36}$. The data in Table 2 also indicate that the calculated singlet–triplet bond length separations for several model silanone compounds, especially those containing an $-\text{OH}$ or $-\text{OSiH}_3$ group, are consistent with the porous silicon photoluminescence excitation spectrum (PLE).

It is noteworthy that the locations of the unsaturated silicon oxyhydride excited triplet states with $-\text{OH}$ or $-\text{OSiH}_3$ moieties and the known peak wavelength of the porous silicon (PLE) excitation spectrum (~ 350 nm)¹³ both bear a clear resemblance to the known singlet–triplet splittings of the low-lying silicon monoxide intercombination band systems³⁶ which occur in a slightly higher energy region. The large changes in the SiO bond lengths indicated in Table 2 in turn produce a large shift in the excited state potentials relative to the ground state, consistent with a significant difference in the peak of the PLE excitation spectrum (~ 350 nm) and the observed PL emission spectrum (~ 500 – 550 nm (green), ~ 600 – 800 nm (orange)). Note that the data in Tables 2 and 3 is consistent with excitation pumping high up the excited state triplet manifold,^{6c,6e,7} with a peak efficiency at wavelengths considerably shorter than 400 nm, followed by subsequent fast vibrational relaxation within the excited state manifold before emission.

There are additional striking trends which are associated with the data of Tables 2 and 3. First, we note that whenever an OH or OSiH_3 (OR) group is bound to the silicon–oxygen bond, the change, $\Delta r(\text{SiO})$, is consistently of order 0.17 Å. Further an additional OH group does little to affect this differential change in bond length accompanying the single–triplet transition. In the absence of an $-\text{OH}$ or $-\text{OR}$ group this change is notably smaller, decreasing from 0.155 Å for $\text{Si}(\text{O})\text{H}_2$ to 0.121 Å for $\text{Si}(\text{O})(\text{SiH}_3)_2$. These are distinct differences associated with an $-\text{OR}$ versus R group bonding to the silicon. Further, we note the very similar adiabatic energy differences, $\Delta E \approx 3.05$ eV, which characterize those singlet–triplet transitions where an OH or OR group is bound to the $\text{Si}=\text{O}$ bond. Contrast these virtually identical energy increments to the much lower and decreasing adiabatic energy differences associated with the

TABLE 4: Select Vibrational Frequencies (cm^{-1}) and Infrared Intensities (km/mol) Calculated for Silanone Ground Electronic States^a

molecule/ assignment	DZP/MP2		DFT/TZVP	
	$\nu(\text{cm}^{-1})$	I (km/mol)	$\nu(\text{cm}^{-1})$	I (km/mol)
$\text{Si}(\text{O})\text{H}_2$				
$\nu(\text{Si}=\text{O})$ stretch	1182	55	1197	67
$\text{Si}(\text{O})\text{H}(\text{SiH}_3)$				
$\nu(\text{Si}=\text{O})$ stretch	1150	26	1178	67
$\text{Si}(\text{O})(\text{SiH}_3)_2$				
$\nu(\text{Si}=\text{O})$ stretch	1125	17	1165	62
$\text{Si}(\text{O})\text{H}(\text{OH})$				
$\nu(\text{Si}=\text{O})$ stretch	1244	135	1245	147
$\nu(\text{Si}-\text{O})$ stretch + ($\text{H}-\text{Si}-\text{O}$ bend + $\text{H}-\text{O}-\text{Si}$ bend)	896	108	869	178
$\text{Si}(\text{O})(\text{OH})_2$				
$\nu(\text{Si}=\text{O})$ stretch	1276	173	1275	194
$\nu(\text{H}-\text{O}-\text{Si})$ bend) sym	921	209	888	186
$\text{Si}(\text{O})\text{H}(\text{OSiH}_3)$				
$\nu(\text{Si}=\text{O})$ stretch dominant	1247	197	1245	185
$\nu(\text{H}-\text{Si}=\text{O})$ bend	905	195	882	69
$\text{Si}(\text{O})(\text{OH})(\text{SiH}_3)$				
$\nu(\text{Si}=\text{O})$ stretch	1222	85	1224	117
$\nu(\text{SiH}_3)$ bend + $\text{H}-\text{O}-\text{Si}$ bend)	886	241	826	168

^a Calculations performed at both the MP2 level with a polarized double- ζ basis set and using a triple- ζ valence basis set at the DFT level (ref 7).

series $\text{Si}(\text{O})\text{H}_2$ ($\Delta r = 0.155 \text{ \AA}$), $\text{Si}(\text{O})\text{H}(\text{SiH}_3)$ ($\Delta r = 0.142 \text{ \AA}$), $\text{Si}(\text{O})(\text{SiH}_3)_2$ ($\Delta r = 0.121 \text{ \AA}$) where the smaller change, $\Delta r(\text{SiO})$, in the SiO bond length will lead to a smaller red shift of the PL emission feature. These results indicate that the oxyhydrides with bound $-\text{OR}$ ligands will produce a much larger red shift of the PL emission spectrum relative to the peak of the PLE excitation spectrum than those fluorophors having only R group ligand binding. We suggest that the magnitudes of these changes are relevant to the correlation of the mechanism for PS formation with the assignment of its transforming green and final orange-red photoluminescence emissions.^{6c} We associate the green emitter with an R group bound fluorophor and the orange emitter with the oxidative insertion into an SiH ($\rightarrow \text{SiOH}$) or $\text{Si}-\text{SiH}_x$ (SiOSiH_x) bond.

Vibrational Spectrum: Comparison with Matrix Isolation Data. Select calculated vibrational frequencies for the considered silanones are given in Table 4.⁷ Here we focus on the $\text{Si}=\text{O}$ stretch frequencies and the ubiquitous 880 cm^{-1} feature. The frequencies calculated for the silanone-based oxyhydrides are quite consistent with the range of frequencies observed in the FTIR spectra^{8–12} as all of the infrared studies indicate the oxidation signaling SiO stretch region and the development of a feature in the $870\text{--}890 \text{ cm}^{-1}$ range. Further the $\nu(\text{Si}=\text{O})$ stretch frequencies calculated for silanone, silanoic acid, and silicic acid, which are given in Table 4, are in excellent agreement with the frequencies determined by Withnall and Andrews²⁸ (1202 cm^{-1} ($\text{Si}(\text{O})\text{H}_2$), 1249 cm^{-1} ($\text{Si}(\text{O})\text{H}(\text{OH})$), and 1270 cm^{-1} ($\text{Si}(\text{O})(\text{OH})_2$) in solid argon matrices as well as the calculation of Kudo and Nagase³⁷ for $\text{H}_2\text{Si}=\text{O}$ (1203 cm^{-1}). The silanones catalogued in Table 5 display clear trends in the calculated $\text{Si}=\text{O}$ stretch region which ranges from 1125 to 1247 cm^{-1} and a dominant $870\text{--}900 \text{ cm}^{-1}$ mode, which when correlated with an OH or OSiH_3 ligand appears to be associated, at least in part, with a combined $\text{Si}-\text{O}$ stretch + $\text{H}-\text{Si}-\text{O}$ ($\text{H}-\text{O}-\text{Si}$) bend. However, we must note that Zacharias et al.¹⁰ have studied the behavior of the 880 cm^{-1} band in hydrogenated amorphous silicon suboxide alloys, finding a minimal dependence on deuteration and therefore ascribing the feature to a

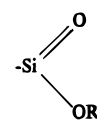
non-hydrogen related origin. The assignment of this mixed mode feature thus appears complex.

The calculated frequency ranges for those silanones catalogued in Table 4 would suggest that not only a $\nu(\text{Si}-\text{O}-\text{Si})$ stretch contributes to the $1050\text{--}1250 \text{ cm}^{-1}$ range but also the $\text{Si}=\text{O}$ stretch. From the trend in the $\text{Si}=\text{O}$ frequency as one traverses the silanones from $\text{Si}(\text{O})\text{H}_2$ to $\text{Si}(\text{O})(\text{SiH}_3)_2$, it is clear that the increased size of the constituency attached to the $\text{Si}=\text{O}$ progressively decreases the $\text{Si}=\text{O}$ stretch frequency such that, in the limit of surface binding, we would anticipate a maximum frequency of order 1125 cm^{-1} for this constituency (taking into account requisite scaling) in the absence of an attached OH or OR group. If an OH or OSiH_3 group replaces a binding H or SiH_3 moiety, the maximum $\text{Si}=\text{O}$ frequency is expected to increase by between 50 and 70 cm^{-1} , still well within the $950\text{--}1250 \text{ cm}^{-1}$ range observed in the FTIR spectrum (Figure 1). We therefore suggest that while the FTIR spectra in this region can be assigned to a surface $\text{Si}-\text{O}-\text{Si}$ mode they might equally well be assigned to the $\text{Si}=\text{O}$ stretch, consistent with the observed PS electronic spectrum. The reassignment of features in this region is also consistent with the observed isotope effect for $^{16}\text{O}/^{18}\text{O}$ given for the experimentally determined 1176 cm^{-1} band in Table 1. If the $\text{Si}=\text{O}$ stretch frequency is 1176 cm^{-1} , consistent with our quantum chemical frequency evaluation, the ^{18}O -substituted frequency should be of order 1134 cm^{-1} , well within the experimental error for the evaluation of the spectral features in Figure 1.

We reassign the spectral features in Figure 1 to a combination of $\text{Si}=\text{O}$ stretch and SiOSi skeletal frequencies. Considering the high potential reactivity of the $\text{Si}=\text{O}$ multiple bond, which is an intermediate that has been previously characterized and stabilized,³⁸ this constituency likely resides only on the PS surface. We have also noted that silanone, silanoic acid, and silicic acid, all of which display $\text{Si}=\text{O}$ bonds, are readily trapped in argon matrices.²⁸ Mawhinney et al. have remarked that the absence of the broad absorbance feature in the $950\text{--}1250 \text{ cm}^{-1}$ region before oxidation suggests that little surface oxide exists on the electrochemically etched PS surface; however, the calculated infrared spectra for the silanones suggest that the summed intensity from the SiH_x absorbance regions can dominate the IR spectrum. Therefore the oxide-based species might require higher concentrations to be observed and their presence in the early stages of the oxidation process may be difficult to evaluate.

Conclusion

We suggest that the photoluminescence excitation spectrum, the photoluminescence emission spectra, and the infrared spectra observed for porous silicon are consistent with the formation of a silanone-based $\text{Si}=\text{O}$ bond. The formation of this $\text{Si}=\text{O}$ bond would appear to be fundamental to the nature of the observed electronic spectrum of the fluorophor bound to the porous silicon surface^{6,7} which, for a photoluminescence excitation spectrum (PLE) peaking at 350 nm and a photoluminescence emission spectrum (PL) in the range $600\text{--}800 \text{ nm}$, we suggest is of the form



where R can be hydrogen (H),⁷ a silyl,⁷ or a hydrocarbon radical.⁵

Acknowledgment. We gratefully acknowledge financial support from the Office of the President at Georgia Institute of

Technology under the auspices of the Focused Research Program. The quantum chemical calculations were performed under the auspices of the Office of Basic Energy Sciences, U.S. Department of Energy under Contract DE-AC06-76RLO 1830 with Battelle Memorial Institute, which operates the Pacific Northwest National Laboratory.

References and Notes

- (1) Canham, L. T. *Appl. Phys. Lett.* **1990**, *57*, 1046.
- (2) Koch, F.; Petrova-Koch, V.; Muschik, T. *J. Lumin.* **1993**, *57*, 271.
- (3) (a) Koch, F.; Petrova-Koch, V.; Muschik, T.; Nikolov, A.; Gavrilenko, V.; *Mater. Res. Soc. Symp. Proc.* **1993**, *283*, 197. (b) Koch, F. *Mater. Res. Soc. Symp. Proc.* **1993**, *298*, 222.
- (4) Prokes, S. M.; *J. Mater. Res.* **1996**, *11*, 305.
- (5) Dudel, F.; Gole, J. L.; Reiger, M.; Bottomley, L. *J. Electrochem. Soc.* To be submitted for publication.
- (6) (a) Dudel, F.; Gole, J. L.; Reiger, M.; Kohl, P.; Pickering, J.; Bottomley, L. *J. Electrochem. Soc.* **1996**, *143*, L164–L166. (b) Dudel, F. P.; Gole, J. L. *J. Appl. Phys.* In press. (c) Gole, J. L.; Dixon, D. A. *J. Phys. Chem.* Submitted for publication. (d) Gole, J. L.; Dudel, Frank P. *J. Appl. Phys.*, in press. (e) Gole, J. L.; Dudel, Frank P.; Grantier, D.; Dixon, David A. *Phys. Rev. B*. In press.
- (7) Gole, J. L.; Dixon, D. A. *Phys. Rev. B*. Submitted for publication.
- (8) Xie, Y. H.; Wilson, W. L.; Ross, F. M.; Mucha, J. A.; Fitzgerald, E. A.; Macauley, J. M.; Harris, T. D. *J. Appl. Phys.* **1992**, *71*, 2403.
- (9) Hory, M. A.; Herino, R.; Ligeon, M.; Muller, F.; Gaspard, F.; Milhalcescu, I.; Vial, J. C. *Thin Solid Films* **1995**, *255*, 200.
- (10) Zacharias, M.; Dimova-Malinouska, D.; Stutzmann, M. *Philos. Mag. B* **1996**, *73*, 799.
- (11) Dubin, V. M.; Ozanam, F. M.; Chazalveil, J. N. *Thin Solid Films* **1995**, *255*, 87–91.
- (12) Mawhinney, D. B.; Glass, J. A., Jr.; Yates, J. T., Jr. *J. Phys. Chem. B* **1997**, *101*, 1202.
- (13) For example, see: Brus, L. E.; Szajowski, P. F.; Wilson, W. L.; Harris, T. D.; Citrin, P. H. *J. Am. Chem. Soc.* **1995**, *117*, 2915.
- (14) For example, see: Calcott, P. D. J.; Nash, K. J.; Canham, L. T.; Kane, M. J.; Brumhead, D. J. *Phys.: Condens. Matter* **1993**, *5*, L91–98.
- (15) Calcott, P. D. J.; Nash, K. J.; Canham, T.; Kane, T. J.; Brumhead, D. J. *Lumin.* **1993**, *57*, 257.
- (16) Nash, K. J.; Calcott, P. D. J.; Canham, L. T.; Needs, R. J. *Phys. Rev. B* **1995**, *51*, 17698.
- (17) (a) Koch, F.; Petrova-Koch, V.; Muschik, T.; Nikolov, A.; Gavrilenko, V.; *Mater. Res. Soc. Symp. Proc.* **1993**, *283*, 197. (b) Koch, F.; Petrova-Koch, V.; Muschik, T.; *J. Lumin.* **1993**, *57*, 271. (c) Koch, F. *Mater. Res. Soc. Symp. Proc.* **1993**, *298*, 222.
- (18) (a) Prokes, S. M.; Glembocki, O. J.; Bermudez, V. M.; Kaplan, R.; Friedersdorf, L. E.; Pearson, P. C. *Phys. Rev. B* **1992**, *45*, 13788. (b) Prokes, S. M. *J. Appl. Phys.* **1993**, *73*, 407.
- (19) Fuchs, H. D.; Rosenbauer, M.; Brandt, M. S.; Ernest, S.; Finkbeiner, S.; Stutzmann, M.; Syassen, K.; Weber, J.; Queisser, H. J.; Cardona, M. *Mater. Res. Soc. Proc.* **1993**, *283*, 203.
- (20) Stutzmann, M.; Brandt, M. S.; Rosenbauer, M.; Fuchs, H. D.; Finkbeiner, S.; Weber, J.; Deak, P. *J. Lumin.* **1993**, *57*, 321.
- (21) Brandt, M. S.; Stutzmann, M. *Solid State Commun.* **1995**, *93*, 473.
- (22) Steckl, A. J.; Xu, J.; Mogul, H. C.; Prokes, S. M. *J. Electrochem. Soc.* **1995**, *142*, L69–71.
- (23) Yan, J.; Shih, S.; Jung, K. H.; Kwong, D. L.; Kovar, M.; White, J. M.; Gnade, B. M.; Magel, L. *Appl. Phys. Lett.* **1994**, *64*, 1374.
- (24) Kern, W.; Puotinen, D. A. *RCA Rev.* **1970**, *31*, 187.
- (25) (a) Andzelm, J.; Wimmer, E.; Salahub, D. R. In *The Challenge of d and f Electrons. Theory and Computation*; Salahub, D. R., Zerner, M. C., Eds.; ACS Symposium Series No. 394; American Chemical Society: Washington, DC, 1989; p 228. (b) Andzelm, J. In *Density Functional Theory in Chemistry*; Labanowski, J., Andzelm, J., Eds.; Springer-Verlag: New York, 1991; p 155. (c) Andzelm, J. W.; Wimmer, E. *J. Chem. Phys.* **1992**, *96*, 1280.
- (26) Frisch, M. J.; Trucks, G. W.; Schlegel, H. B.; Gill, P. M. W.; Johnson, B. G.; Robb, M. A.; Cheeseman, J. R.; Keith, T.; Petersson, G. A.; Montgomery, J. A.; Raghavachari, K.; Al-Laham, M. A.; Zakrzewski, V. G.; Ortiz, J. V.; Foresman, J. B.; Cioslowski, J.; Stefanov, B. B.; Nanayakkara, A.; Challacombe, M.; Peng, C. Y.; Ayala, P. Y.; Chen, W.; Wong, M. W.; Andres, J. L.; Replogle, E. S.; Gomperts, R.; Martin, R. L.; Fox, D. J.; Binkley, J. S.; Defrees, D. J.; Baker, J.; Stewart, J. P.; Head-Gordon, M.; Gonzales, C.; Pople, J. A. *Gaussian 94*, Gaussian, Inc.: Pittsburgh, PA, 1995.
- (27) Prokes, S. M. *Electrochem. Soc. Interface*, **1994**, *3*, 41–43.
- (28) For a matrix infrared study also see: Withnall, R.; Andrews, L. *J. Phys. Chem.* **1985**, *89*, 3261.
- (29) Godbout, N.; Salahub, D. R.; Andzelm, J.; Wimmer, E. *Can. J. Chem.* **1992**, *70*, 560.
- (30) Komoricki, A.; Fitzgerald, G. *J. Phys. Chem.* **1993**, *98*, 1398 and references therein.
- (31) (a) Moller, C.; Plesset, M. S. *Phys. Rev.* **1934**, *46*, 618. (b) Pople, J. A.; Binkley, J. S.; Seeger, R. *Int. J. Quantum Chem., Quantum Chem. Symp.* **1976**, *10*, 1.
- (32) Dunning, T. H., Jr.; Hay, P. J. In *Methods of Electronic Structure Theory*; Schaefer, H. F., III, Ed.; Plenum Press: New York, 1977; Chapter 1. McLean, A. D.; Chandler, G. S. *J. Chem. Phys.* **1980**, *72*, 5639.
- (33) (a) Bartlett, R. J. *J. Phys. Chem.* **1989**, *93*, 1697. (b) Kucharski, S. A.; Bartlett, R. J. *Adv. Quantum Chem.* **1986**, *18*, 281. (c) Bartlett, R. J.; Stanton, J. F. In *Reviews of Computational Chemistry*; Lipkowitz, K. B., Boyd, D. B., Eds.; VCH Publishers: New York, 1995; Vol. V, Chapter 2, p 65.
- (34) For the Si basis, see: Dobbs, K. D.; Dixon, D. A. *J. Phys. Chem.* **1994**, *98*, 5290. For O and H, see: Dobbs, K. D.; Dixon, D. A.; Kornonicki, A. *J. Chem. Phys.* **1993**, *98*, 8852.
- (35) Hedelund, L. *Astrophysic. Lett.* **1972**, *11*, 71.
- (36) For example, see Green, G. J.; Gole, J. L. *Chem. Phys.* **1985**, *100*, 133.
- (37) Kudo, T.; Nagase, S. *Chem. Phys. Lett.* **1986**, *128*, 507.
- (38) Maltsev, A. E.; Khabashesku, V. N.; Nefedov, O. N.; Zelinsky, N. D. Intermediates with Si=O multiple bond: generation, stabilization, and direct spectroscopic study. *Proceedings of the 8th International Symposium on Organosilicon Chemistry*, St. Louis, Missouri, June 7–12, 1987; Halsted Press: New York, 1988.